

# Neural Correlates of Visual Working Memory: fMRI Amplitude Predicts Task Performance

Luiz Pessoa,<sup>1</sup> Eva Gutierrez, Peter A. Bandettini,  
and Leslie G. Ungerleider

Laboratory of Brain and Cognition  
National Institute of Mental Health  
National Institutes of Health  
Bethesda, Maryland 20892

## Summary

We used fMRI to investigate how moment-to-moment neural activity contributes to success or failure on individual trials of a visual working memory (WM) task. We found that different nodes of a distributed cortical network were activated to a greater extent for correct compared to incorrect trials during stimulus encoding, memory maintenance during delays, and at test. A logistic regression analysis revealed that the fMRI signal amplitude during the delay interval in a network of frontoparietal regions predicted successful performance on a trial-by-trial basis. Differential delay activity occurred even for only those trials in which BOLD activity during encoding was strong, demonstrating that it was not a simple consequence of effective versus ineffective encoding. Our results indicate that accurate memory depends on strong sustained signals that span the delay interval of WM tasks.

## Introduction

Working memory (WM) refers to the process of actively maintaining relevant information in mind for brief periods of time. In a typical WM paradigm, on each trial, a sample stimulus is presented, followed by a delay of several seconds, and then a test stimulus is shown. The subject's task is to indicate whether or not the test stimulus matches the sample. This type of WM task requires primarily maintenance operations, in which the short-term memory store is emptied after each trial.

WM has been extensively investigated in monkeys, where the importance of prefrontal regions has been established. Lesions of the dorsolateral prefrontal cortex, especially within and surrounding the principal sulcus (Brodmann area [BA] 46), greatly impair WM performance (Bauer and Fuster, 1976; Funahashi et al., 1993; Goldman and Rosvold, 1970). At the same time, results from single-cell studies have demonstrated that prefrontal neurons show stimulus-specific sustained discharge during the delay period (Fuster and Alexander, 1971; Kubota and Niki, 1971; for reviews, see Fuster, 1997; Goldman-Rakic, 1995). This sustained activity has been interpreted to be the neural correlate of maintenance processes that take place during the delay and thus has been taken to be the neural signature of WM (Fuster, 2001). Sustained activity during the delay interval is not confined, however, to the prefrontal cortex. Depending

on the type of stimulus, cells with sustained responses have been found in the inferior temporal cortex (for visual patterns or color stimuli; Chelazzi et al., 1998; Fuster and Jervey, 1982), the parietal cortex (for visuospatial stimuli; Chafee and Goldman-Rakic, 1998, 2000), and the premotor cortex (for particular motor responses; Bruce and Goldberg, 1985).

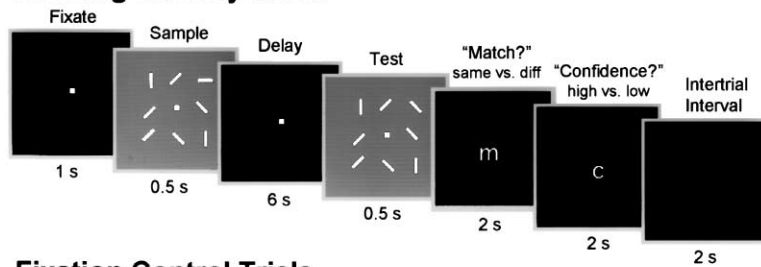
In tasks similar to those used in monkeys, functional brain imaging studies in humans have also provided evidence supporting the role of prefrontal regions in WM by demonstrating sustained signals during delay intervals (Cohen et al., 1997; Courtney et al., 1997; for review, see D'Esposito, 2001). The prefrontal regions that show this activity include the middle frontal gyrus (BA 9/46), thought to be the human homolog of the principal sulcal region of dorsolateral prefrontal cortex in monkeys, as well as more ventral regions in the inferior frontal gyrus (BA 44, 45, 47). As in monkeys, several studies in humans have shown that regions outside of prefrontal cortex also exhibit sustained delay activity, including the inferior temporal cortex (Courtney et al., 1998), the parietal cortex (D'Esposito et al., 1998; Jonides et al., 1998; Rowe et al., 2000), and the premotor cortex (Courtney et al., 1998; Petit et al., 1998).

What determines successful performance in a WM task? Results from single-cell studies help clarify how neural activity may contribute to behavioral performance. It has been reported that, on trials in which monkeys make errors, activity during the delay interval fails to be sustained (Funahashi et al., 1989; Fuster, 1973; Rosenkilde et al., 1981; Watanabe, 1986a, 1986b), suggesting that activity during the delay bridges the gap between the sample and test stimuli to enable monkeys to correctly match them. However, the precise relationship between delay activity and performance is not yet known. For example, in single-cell studies the analysis of error trials has been problematical due to the very limited number of such trials. Monkeys are typically trained to perform at very high levels of performance (90% correct or higher), such that only very few error trials are typically available for a given cell (but see Fuster et al., 2000), which has usually precluded a quantitative assessment of the relationship between neuronal firing during WM delays and behavioral performance. Additionally, in single-cell studies, it is possible that for incorrect trials the monkey never encoded the sample stimulus effectively, which in turn would lead to reduced neural activity during the delay. Finally, for neural activity to be a critical substrate of WM, it should be maintained during the entire delay period when associated with successful performance. Thus, cells whose sustained activity is interrupted by distracting stimuli cannot play a necessary role in WM (Miller et al., 1996) if, on those trials, the monkey continues to perform the task correctly. In this case, sustained activity elsewhere in the brain presumably provides the neural substrate for WM.

To investigate the neural substrates of WM performance on a trial-by-trial basis, it is instructive to decompose a WM trial into three phases, namely, encoding, delay, and test. The encoding phase includes the per-

<sup>1</sup>Correspondence: pessoa@ln.nimh.nih.gov

## Working Memory Trials



## Fixation Control Trials

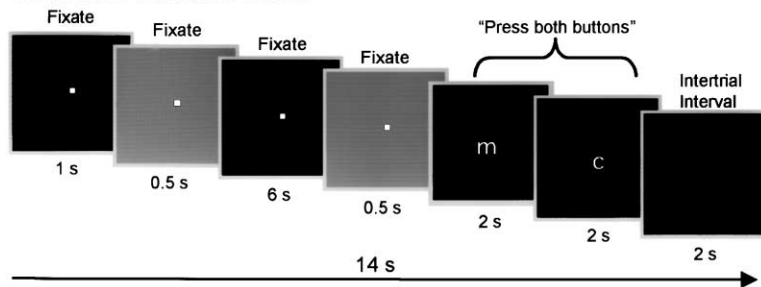


Figure 1. Experimental Design

Two types of trials were employed: working memory (WM) and fixation control (FC). In WM trials, subjects indicated whether the sample and test displays were the same or different (note that the bar orientation on the upper right changed in the present case). They also indicated the confidence of their response (high versus low). FC trials did not have any memory maintenance requirements, and subjects pressed both buttons at both response periods.

ceptual processing of the sample stimulus; the delay phase includes the processes that actively maintain the sample item in short-term memory; and the test phase includes the perceptual processing of the test stimulus, matching the test stimulus to the sample stimulus, as well as preparatory response processes. For a WM trial to be correct, the neural processes occurring during all three task phases must be executed successfully. Because, in general, cells are not tuned to all task phases, it has not been possible in physiological studies to assess, at the same time, the contributions of activity during the different task components to WM performance. By contrast, using functional magnetic resonance imaging (fMRI), BOLD signals across the entire network of areas engaged by WM can be evaluated simultaneously during each task phase.

In the present study, we investigated how the moment-to-moment activity within cortical regions, as measured by fMRI, contributes to success or failure on individual trials of a WM task. Specifically, we examined how the entire network of regions engaged in visual WM was differentially activated during trials that led to correct and incorrect outcomes. We hypothesized that different components of the task, namely, encoding, delay, and test, would engage different nodes of the WM network to a greater extent on correct trials compared to incorrect trials and provide the neural correlates of WM performance. In particular, we hypothesized that BOLD activity during the delay interval would be stronger and more sustained on correct than on incorrect trials and would thus predict task performance. Moreover, we anticipated that this would be the case even if one examined only those trials that showed evidence of effective encoding of the sample stimulus.

## Results

Nine subjects were scanned as they performed two types of trials: working memory (WM) and fixation control (FC) (Figure 1; Experimental Procedures). WM trials,

each lasting 14 s, consisted of 1 s of fixation, a sample visual display for 0.5 s, a 6 s delay period, a test display for 0.5 s, two response periods of 2 s each, and finally an intertrial interval with a blank screen for 2 s. The sample and test displays consisted of a fixation spot and an array of eight oriented white bars on a gray background. During the two response periods, subjects indicated with a right or left button press, first, whether or not the test display matched the sample display (a nonmatch meant a single bar in the display changed its orientation) and, second, the confidence of their decision ("high" or "low"). In each run, half of the WM trials involved a change in the display, and half did not. FC trials did not have any maintenance requirements, and subjects simply maintained fixation and pressed both buttons during both response periods. All analyses reported below employed high-confidence trials only; in this manner we attempted to minimize the contributions of guess trials (cf. Brewer et al., 1998; Wagner et al., 1998).

We analyzed the results in two complementary ways (Experimental Procedures). First, regions of interest (ROIs) were selected independent of task performance, and then differences in activity within these regions for correct and incorrect trials were evaluated at the group level, using a random-effects analysis. These results were supplemented with a fixed-effects analysis performed on a voxel-wise manner in order to generate summary group Z maps. Although less exacting than a random-effects analysis, it provided a summary description of whole-brain activation for the group of subjects studied herein.

## Behavioral Results

For WM trials, mean performance across subjects was 71.4% correct for high-confidence trials. On these trials, no significant difference in reaction times was observed for correct or incorrect trials (mean  $\pm$  SD; correct, 899  $\pm$  138 s; incorrect, 936  $\pm$  181 s;  $p > 0.05$ ,  $t$  test). For the low-confidence trials, mean performance dropped to

Table 1. Performance Index Values of Brain Regions Involved in Visual Working Memory

Region	Hemisphere	Performance Index <sup>a</sup>			Talairach Coordinates			Brodmann Area
		Encoding	Delay	Test	X	Y	Z	
Pre-SMA			*(1.51)	** (0.41)	1	7	48	6
Anterior cingulate				*(0.72)	-3	24	31	32
FEF/superior frontal sulcus	L		** (0.94)		-25	-9	48	6/8
	R	*(1.01)	*(0.93)		25	-7	48	6/8
Precentral sulcus at posterior MFG	L			*(0.46)	-44	1	28	6/9
	R			*(0.58)	44	1	33	6/9
DLPFC	L	*(0.75)	*(1.47)	*(0.56)	-37	28	30	9/46
	R	*(0.91)			43	34	27	9/46
Anterior insula	L			** (0.60)	-31	20	8	44/45
	R			** (0.57)	32	20	9	44/45
SPL (posterior parietal)	L	** (0.81)	** (0.85)		-22	-61	43	7
	R	** (0.78)	*(0.86)		18	-67	45	7
IPS (anterior parietal)	L	*(0.73)	** (1.13)		-38	-43	39	40
	R	*(0.68)	*(1.10)		38	-37	36	40
Inferior temporal gyrus	L				-43	-60	-11	37
	R			** (0.43)	50	-52	-12	37
Dorsal occipital	L	*(0.69)	** (0.95)		-32	-79	9	18/19
	R	*(0.62)			29	-82	8	18/19
Posterior calcarine				*(0.56)	-3	-87	-3	17/18

Statistical tests (random-effects analysis): single asterisk (\*) indicates  $p < 0.05$ ; double asterisk (\*\*) indicates  $p < 0.01$ . DLPFC, dorsolateral prefrontal cortex; FEF, frontal eye field; IPS, intraparietal sulcus; MFG, midfrontal gyrus; SMA, supplementary motor area; SPL, superior parietal lobule.

<sup>a</sup> The performance index (values in parentheses) was defined as the normalized difference between the  $\beta$  weights for correct and incorrect trials at each task phase.

60.8% correct, indicating that indeed guessing came into play on these trials.

### Working Memory Network

We first isolated the entire network of regions involved in WM independent of performance by comparing BOLD activity for WM and FC trials. The main regions revealed by this contrast are listed in Table 1. These regions include dorsal occipital, inferior temporal, parietal, as well as premotor and prefrontal cortex, as illustrated on a surface rendering of the left and right hemispheres in Figure 2.

Having isolated the WM network, we then probed how it was differentially activated according to task performance. This was accomplished by comparing BOLD activity on correct trials and incorrect trials during each task phase, namely, encoding, maintenance, and test.

several areas it was modulated during more than one phase.

### Performance-Related BOLD Activity: Correct versus Incorrect Trials

#### Encoding

The comparison of BOLD signals for correct versus incorrect trials at encoding revealed performance-related activity in extrastriate regions that were involved in the visual processing of the stimulus display (Figure 3A). These regions included the dorsal occipital cortex in the middle occipital gyrus (BA 18/19) and the inferior temporal cortex (BA 37); in some subjects, the latter activation was located in the inferior temporal gyrus, but in others, it shifted ventrally to the fusiform gyrus. For both the dorsal occipital and inferior temporal regions, the activations were bilateral (for these regions and all others listed below Table 1 indicates those that survived the random-effects analysis). Outside visual

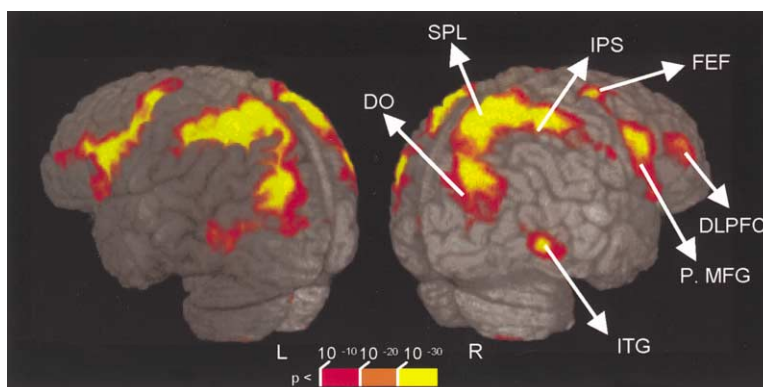
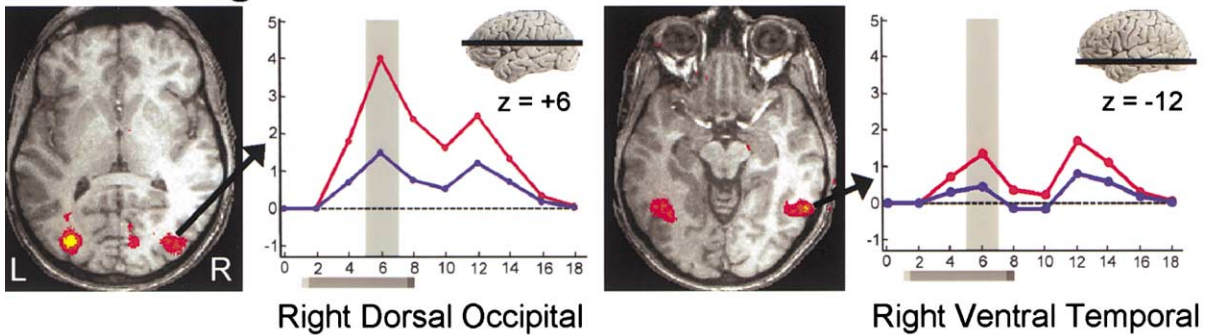


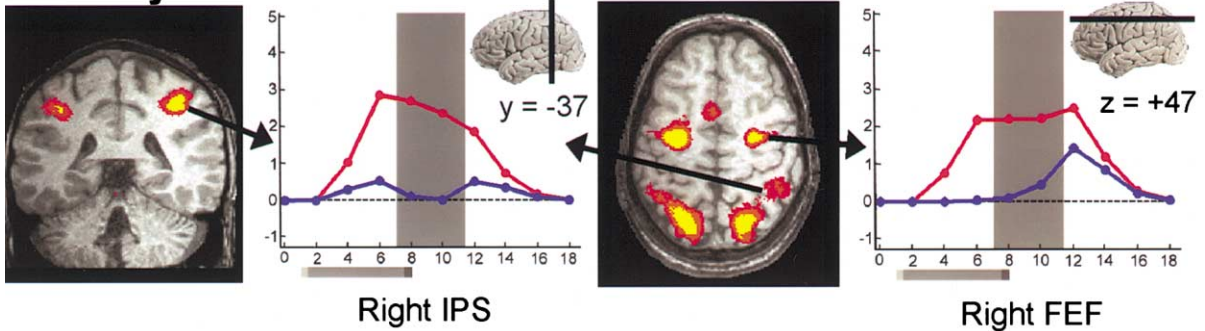
Figure 2. Working Memory Network

The regions within this network were revealed by the contrast of working memory versus fixation control trials. The statistical group maps of functional activations are shown overlaid onto a three-dimensional rendering of the brain of a representative individual. The color bar indicates  $p$  values (uncorrected). DLPFC, dorsolateral prefrontal cortex; DO, dorsal occipital; FEF, frontal eye field; IPS, intraparietal sulcus; ITG, inferior temporal gyrus; P. MFG, posterior middle frontal gyrus; SPL, superior parietal lobule.

## A. Encoding



## B. Delay



## C. Test

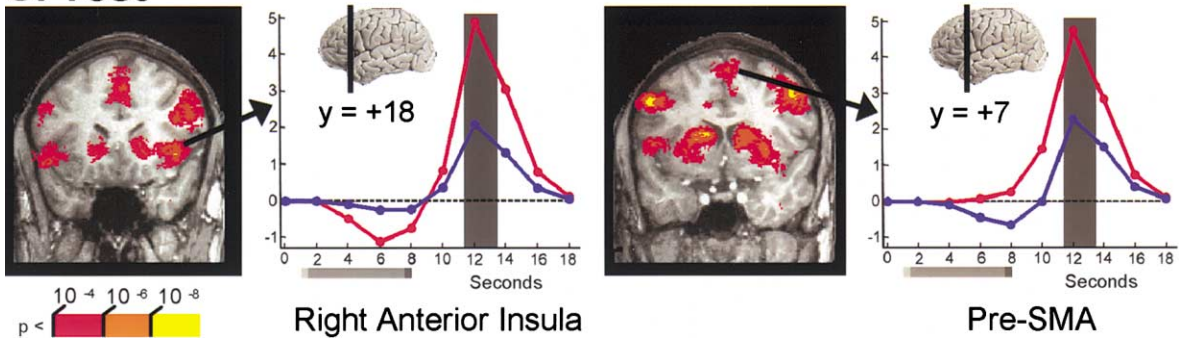


Figure 3. Performance-Related Activity during the Three Phases of the Working Memory Task: Encoding, Delay, and Test

Performance-related activity was obtained by comparing activity for correct and incorrect trials at each task phase. Functional group maps are shown overlaid onto structural scans from a representative individual. Arrows indicate the region from which the fitted hemodynamic responses were obtained, which were estimated by comparing the responses to correct (red) and incorrect (blue) trials with multiple regression. The color bar indicates  $p$  values (uncorrected). The level of the axial and coronal sections is indicated on the small whole-brain insets. The bar below each  $x$  axis codes the periods when the sample stimulus (light gray), the delay (intermediate gray), and the test stimulus (dark gray) occurred during the task. The vertical gray bars for encoding and test are centered 5 s after the stimulus presentation; the gray bar for delay was centered between the latter two bars. (A) Performance-related activity at encoding included dorsal occipital cortex and inferior temporal extrastriate cortex, visual areas sensitive to the sample stimulus. (B) Performance-related activity during the delay included the right IPS in anterior parietal cortex and the right FEF. (C) Performance-related activity at test occurred in a wide network of regions, including the right anterior insula and the presupplementary motor area (pre-SMA). For a complete list of regions showing significant performance-related activity, see Table 1. Abbreviations are as in Figure 2.

cortex, we observed differential activity in parietal and frontal regions, including superior parietal lobule (SPL; BA 7) within posterior parietal cortex, the cortex along the intraparietal sulcus (IPS; BA 40) within anterior parietal cortex, dorsolateral prefrontal cortex (DLPFC; BA 9/46), and frontal eye field (FEF; BA 6/8). The calcarine fissure (V1/V2; BA17/18) also showed transient differential activity. Subcortically, the right thalamus and right caudate showed differential performance-related BOLD activity during encoding.

### Delay Interval

The comparison of BOLD signals for correct versus incorrect trials during the delay interval revealed significant performance-related BOLD activity in parietal and frontal cortex, which was characterized by robust sustained signals on the correct trials (Figure 3B). The regions showing this effect included the DLPFC, SPL, IPS, FEF (the activation extended forward from the FEF within the precentral sulcus [BA 6] to include the most posterior portion of the superior frontal sulcus [BA 8]), and the

dorsal occipital cortex. The presupplementary motor area (Pre-SMA; BA 6) also exhibited differential activity during the delay. As Table 1 shows, the large majority of these regions also showed differential activity at encoding.

Other regions differentially activated in our voxel-wise maps (fixed-effects analysis) for correct versus incorrect trials included the precentral sulcus at the posterior aspect of the middle frontal gyrus (MFG) bilaterally (BA 6/9), the anterior cingulate gyrus bilaterally (BA 32), and the right hippocampus/parahippocampal gyrus (BA 28). Subcortically, no structure showed differential performance-related BOLD activity during the delay interval.

### Test

Several regions significantly activated on WM relative to FC trials also showed greater BOLD activity for correct than incorrect trials at test. These differentially activated regions ranged from very early visual areas in posterior cortex to anterior prefrontal regions (Table 1). Figure 3C shows two of these areas, namely, the anterior insula bilaterally (BA 44/45) and the pre-SMA. Other regions exhibiting differential BOLD activity at test included the calcarine fissure, the inferior temporal gyrus, DLPFC, posterior MFG, and anterior cingulate. The main subcortical structures that showed differential performance-related BOLD activity during retrieval were the caudate and putamen (Figure 3C), the cerebellum and the pulvinar, mainly on the right.

### fMRI Signal Amplitude and Subjects' Performance

To quantify the contributions of BOLD activity to behavioral performance, we computed a performance index for each ROI during each phase of the WM task (Experimental Procedures). This index provided a normalized difference between the  $\beta$  weights for correct and incorrect trials during each task phase. The performance index, averaged across subjects for every significant ROI, was 0.77 for encoding, 1.08 for delay, and 0.54 for test (Table 1) and was significantly greater than zero in all cases (one-tailed  $t$  test,  $p < 0.05$ ). All task phases differed from each other as assessed by post-hoc Newman-Keuls tests (in all cases  $p < 0.005$ ).

To further quantify the relationship between fMRI signal amplitude and the subjects' performance, we employed a logistic regression analysis. We fit a logistic function to the subjects' performance on each trial as a function of the fMRI signal amplitude on that trial (Experimental Procedures). The slope of the best-fitting logistic function measures the strength of the predictive effect of fMRI signal amplitude for behavioral performance. We measured the strength of the predictive effect for every time-point within a trial for those ROIs exhibiting significant performance-related BOLD activity during the delay according to the random-effects analysis (Table 1). For all subjects combined, BOLD activity between 8 to 12 s reliably predicted behavioral performance for all ROIs listed in Table 1, the single exception being the left dorsal occipital cortex. Specifically, the best-fit slope was reliably greater than zero ( $p < 0.05$ ) for the right and left SPL and FEF at 8 and 10 s; for the right and left IPS at 8, 10, and 12 s; and for the left DLPFC and the Pre-SMA at 10 s. As shown in

Figure 4, a 1% increase in amplitude of fMRI signal increased the probability of being correct on that trial from chance to close to 70% for the right IPS and right FEF and close to 65% for the left DLPFC.

Although it was found that activity at 8, 10, and 12 s reliably predicted performance, it is difficult to definitively assign this activity to a distinct task phase because of the large overlap of phase-related hemodynamic responses during the trial. Nevertheless, if one assumes roughly a 5 s lag for the hemodynamic response to peak (Bandettini, 1999; Cohen, 1997), then BOLD activity evoked by the sample stimulus should peak at about 6 s, and BOLD activity evoked by the test stimulus should peak at about 12.5 s. Therefore, we suggest that activity at 8–10 s largely reflects maintenance processes occurring during the delay interval. The sharp drop in predictability in the right FEF at test is consistent with the relatively strong BOLD signal in this region for incorrect trials during this task phase (see Figure 3B, right).

### Encoding and Delay Signals and Successful Performance

Most regions exhibiting differential BOLD activity for correct relative to incorrect trials during the delay also exhibited an encoding effect (see Table 1). Therefore, an important question is whether, for incorrect trials, subjects encoded the sample stimulus effectively. If not, then weak delay signals may have been a simple consequence of the lack of effective encoding. This possibility is difficult to completely eliminate because it depends on the proper determination of what constitutes "effective" or "strong" encoding. Ideally, one would like to demonstrate that even on trials in which effective encoding took place, BOLD delay activity remained a significant predictor of correct performance. We handled this difficult issue in the following manner. First, we employed "high confidence" trials, which may have helped to minimize the contribution of "weakly encoded events." Second, we performed additional analyses confined to only those trials with strong BOLD signals at encoding (see Experimental Procedures), with results virtually identical to the ones shown in Figure 3B. Moreover, a random-effects analysis revealed that all ROIs with significant contributions to correct performance during the delay (Table 1) were also significant when the analysis was restricted to only the effectively encoded trials (in all cases  $p < 0.05$ ).

We further investigated the relationship between encoding and delay signals by examining the distribution of delay signals for effectively encoded trials separately for correct and incorrect trials. Figure 5 illustrates that for the right IPS, right FEF, and left DLPFC (the regions shown in Figure 4), the distribution for correct trials was skewed to the right relative to incorrect trials, indicating that on these trials BOLD delay activity was significantly greater for correct than for incorrect trials (one-tailed  $t$  test; in all cases  $p < 0.005$ ). Moreover, logistic regressions on the delay signals of trials with strong encoding indicated that delay activity reliably predicted performance for these three ROIs (in all cases  $p < 0.01$ ); a 1% increase in amplitude of fMRI signal increased the probability of being correct on that trial from chance to 72% in the right IPS and FEF and to 70% in the left



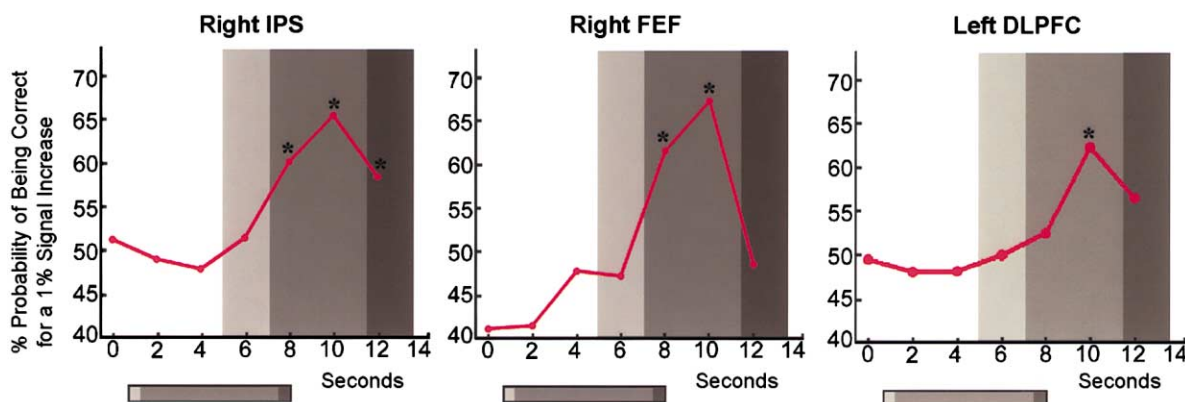


Figure 4. fMRI Signal Amplitude Predicts Subjects' Performance

The contingency between fMRI signal amplitude and the subjects' performance was assessed with a logistic regression analysis for every time point within working memory trials. (Left panel) For the right IPS, activity at 8, 10, and 12 s significantly predicted performance (asterisks denote  $p < 0.05$ ). (Middle panel) For the right FEF, activity at 8 and 10 s significantly predicted performance. For both these ROIs, for a 1% increase in BOLD signal, the probability of being correct for that trial increased from chance to close to 70%. (Right panel) For the left DLPFC, activity at 10 s significantly predicted performance. The inset below the x axes and the shaded vertical bars are as in Figure 3. Note that, for the regions shown, the fMRI signal during the delay interval significantly predicted the outcome on a trial-by-trial basis. Abbreviations are as in Figure 2.

DLPFC, indicating improved predictability for strongly encoded trials relative to the situation in which all trials are considered. At the same time, for weakly encoded events, the distributions of delay activity for correct and incorrect trials did not differ from each other for the right FEF and left DLPFC; for the right IPS, delay activity was significantly greater for correct than incorrect trials (one-tailed  $t$  test,  $p < 0.001$ ). For weakly encoded events, delay activity did not predict performance for the right FEF and left DLPFC, as revealed by logistic regressions; for the right IPS, delay activity still predicted performance ( $p < 0.001$ ; a 1% increase in fMRI amplitude increased the probability of being correct to 67%; note that this constitutes a reduction of 5% from that ob-

tained for strongly encoded trials). Finally, we investigated the distribution of encoding signals for correct and incorrect trials for the visual area with the strongest differential signal at encoding, namely, the left dorsal occipital area. For effectively encoded trials, BOLD activity at encoding in this region did not differ significantly between correct and incorrect trials. Moreover, a logistic regression was not statistically significant.

#### Parietofrontal Coupling for Correct versus Incorrect Trials

To probe how brain regions interacted as subjects performed the WM task, we next investigated how brain regions were coupled during both correct and incorrect

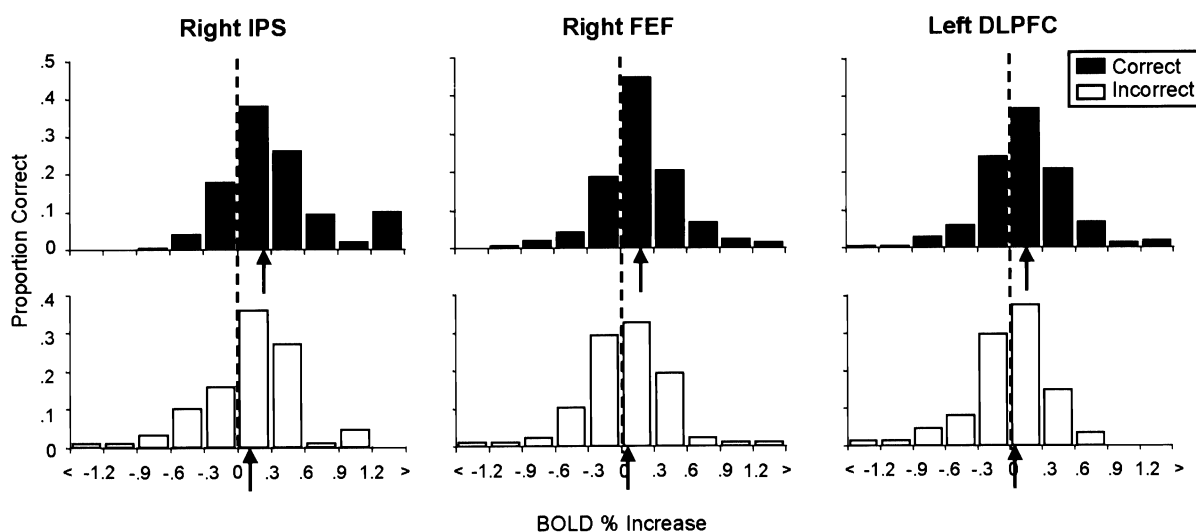


Figure 5. Distribution of Delay Signals for Correct and Incorrect Strongly Encoded Trials

In all cases, the distribution for correct trials was skewed to the right relative to incorrect trials, showing that, on these trials, BOLD activity was significantly greater for correct than incorrect trials (one-tailed  $t$  test; in all cases  $p < 0.005$ ). Arrows point to the mean of the distributions. Abbreviations are as in Figure 2.

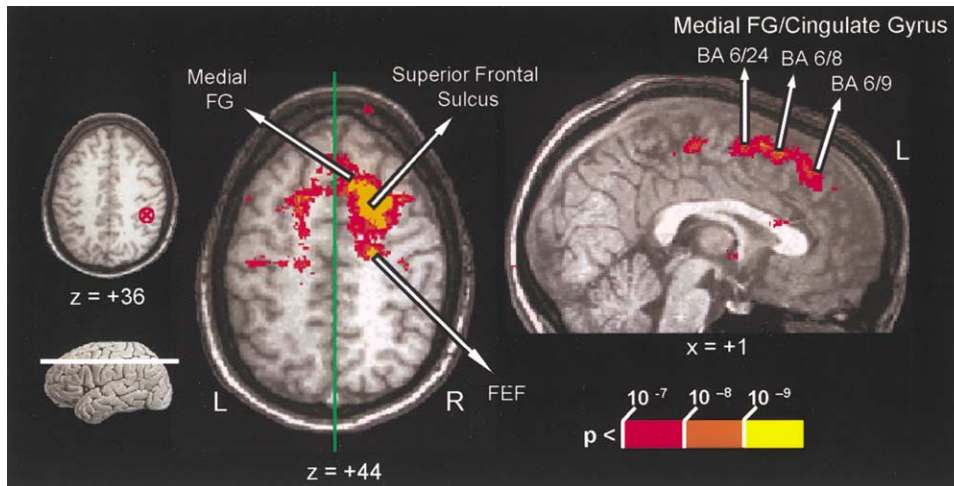


Figure 6. Increases in Parietofrontal Activity Coupling on Correct Compared to Incorrect Trials

Performance-related increases in “functional connectivity” with the right IPS (inset at top left) included the frontal eye field, the superior frontal sulcus, and the medial frontal/cingulate gyrus, as shown on the axial and sagittal sections. The green line on the axial section indicates the level of the sagittal section, and the white line on the small brain (inset at lower right) indicates the level of the axial section. The color bar indicates p values (uncorrected).

trials by testing for performance-dependent changes in “functional connectivity” during the delay interval (Friston et al., 1997). This analysis highlights changes in the coupling between brain regions, i.e., the contribution of one area to the signal measured in a different area as a function of experimental condition (in this case, behavioral performance). In this analysis, we were interested in increases in the correlation of the signals between two areas when comparing incorrect and correct trials. We tested for any such increase in functional connectivity with the right IPS cortex ( $x = 38$ ,  $y = -37$ ,  $z = 36$ ). We chose this region because it not only exhibited strong delay-related activity in our task but also has been shown to be functionally coupled with prefrontal cortex in single-cell studies (Chafee and Goldman-Rakic, 2000; see also Discussion). The results showed significant effects in the right frontal cortex, including the FEF and cortex anterior to it (Figure 6). More specifically, an increase in correlated BOLD activity on correct compared to incorrect trials with the right IPS was found (1) in the right FEF (BA 6;  $x = 24$ ,  $y = -10$ ,  $z = 47$ ), extending forward in the superior frontal sulcus from BA 6 to BA 8 (from  $x = 18$ ,  $y = 3$ ,  $z = 44$  to  $x = 19$ ,  $y = 19$ ,  $z = 44$ ); (2) along the medial frontal gyrus, extending from posterior (BA 6/24; right:  $x = 1$ ,  $y = -1$ ,  $z = 50$ ; left:  $x = -1$ ,  $y = -1$ ,  $z = 50$ ) to anterior sites (BA 6/9/32; right:  $x = 1$ ,  $y = 36$ ,  $z = 32$ ; left:  $x = -1$ ,  $y = 36$ ,  $z = 32$ ); (3) in the right cuneus (BA 19;  $x = 11$ ,  $y = -82$ ,  $z = 36$ ); and (4) in the left middle occipital gyrus ( $x = -25$ ,  $y = -67$ ,  $z = 9$ ). Of these sites, the random-effects analysis showed that the FEF/superior frontal sulcus region also showed significant differential performance-related BOLD activity during the delay interval (Table 1).

## Discussion

In the present study, we explored the neural substrates of WM performance on a trial-by-trial basis using fMRI. To do so, we first defined the WM network independent

of the subjects’ response and then probed nodes of this network for performance-related BOLD activity. Our results demonstrated that different nodes were activated to a greater extent for correct compared to incorrect trials during distinct components of the task, namely, encoding, delay, and test. Additionally, as we anticipated, signals during the delay interval were both stronger and more sustained for correct compared to incorrect trials. Moreover, a logistic regression analysis revealed that fMRI signal amplitude during the delay interval predicted successful performance on a trial-by-trial basis.

## Role of Maintenance Activity for WM Performance

To quantify the contributions of BOLD activity during the encoding, delay, and test phases of the task to behavioral performance, we employed a performance index, which assessed the increase in activity for correct compared to incorrect trials. Regions exhibiting differential BOLD activity during the delay were almost exclusively in frontal and parietal cortex and included the DLPFC, FEF, SPL, IPS, and Pre-SMA. We further quantified the relationship between fMRI signal amplitude and performance using a logistic regression analysis. This analysis revealed that the strength of the fMRI signal during the delay interval reliably predicted task performance: for example, a 1% increase in signal in the right IPS and FEF increased the likelihood of success to close to 70%, and in the left DLPFC to close to 65%. Moreover, for strongly encoded trials, the probability increased to 72% in the right IPS and FEF and to 70% in the left DLPFC. Taken together, the results provide direct evidence linking sustained activity during the delay interval with behavioral success on a trial-by-trial basis.

The importance of sustained activity for WM performance is consistent with previous evidence from single-cell studies. These studies showed that delay-related neural activity on incorrect trials was weak or absent, suggesting that the level of firing during the delay inter-

val may correlate with behavioral performance (Funahashi et al., 1989; Fuster, 1973; Rosenkilde et al., 1981; Watanabe, 1986a, 1986b). Our study extends these results by quantifying the contribution provided by sustained activity during the delay as inferred from fMRI signals and by demonstrating that this activity is required for successful performance. Consistent with the physiological results, for most regions, delay signals on incorrect trials were not significantly different from zero (as assessed by a *t* test on the  $\beta$  weights of the delay component of incorrect trials;  $p > 0.05$ ); the two exceptions were the Pre-SMA and the SPL bilaterally, where delay activity was significantly greater than zero ( $p < 0.05$ ), though reduced compared to correct trials.

Both single-cell and lesion studies in monkeys have demonstrated that the DLPFC (BA 9/46) is centrally involved in WM (Fuster, 1997; Goldman-Rakic, 1995), and in humans the corresponding region is commonly activated in WM tasks (for reviews, see Cabeza and Nyberg, 2000; D'Esposito, 2001). Here we show not only that the DLPFC is involved in WM but also that its contribution to correct performance is significant. Recently, it has been shown that strong DLPFC BOLD signals during delay periods help overcome the potentially deleterious effects of intervening distracters in a WM task (Sakai et al., 2002), consistent with single-cell findings (Miller et al., 1996).

Another region that showed a significant contribution of sustained delay signals for WM performance included FEF in the precentral sulcus extending forward into the superior frontal sulcus (BA 6/8). Several imaging studies have revealed WM-related activity in the vicinity of the precentral sulcus and the superior frontal sulcus. Although such activity has often been attributed to hand or eye movements within premotor cortex, WM studies that have explicitly controlled all motor responses have also observed activations in this region (Courtney et al., 1996; Jonides et al., 1993; Smith et al., 1995). Critically, sustained activity has been demonstrated in the superior frontal sulcus during the delay interval of WM tasks (Courtney et al., 1998; Postle et al., 2000a), and this activity appears to be greater for spatial than for object WM (Courtney et al., 1998).

Within parietal cortex, bilateral SPL (BA 7) and IPS (BA 40) also exhibited differential delay signals. This finding is consistent with previous imaging work demonstrating SPL activation associated with both spatial and verbal WM tasks and IPS activation with object WM tasks as well (for reviews, see Cabeza and Nyberg, 2000; D'Esposito, 2001). Recently, Rowe et al. (2000) have suggested that the posterior IPS may be especially important for maintenance processes, as it exhibited sustained activity over WM delays up to 18.5 s.

Finally, we found performance-related delay signals in the Pre-SMA. The Pre-SMA is thought to participate in cognitive operations that precede motor output, such as the selection of and preparation for motor responses (Picard and Strick, 1996). The Pre-SMA has also been found to exhibit sustained BOLD activity during both spatial and face WM tasks (Petit et al., 1998). We found greater BOLD activity for correct versus incorrect trials at the end of the delay interval in Pre-SMA. Thus, it is possible that the sustained activity we observed here

may be related to a state of preparedness to select a response based on information that is held in WM.

There is evidence that areas in frontal and parietal cortex interact functionally during WM tasks. Chafee and Goldman-Rakic (2000) recorded neuronal activity in monkey prefrontal cortex (area 8a which includes the FEF) while parietal cortex was cooled and in parietal cortex (the lateral bank of the IPS) while prefrontal cortex was cooled. The effects of cooling the two regions were essentially equivalent, producing an average change in activity of about 40%. These findings thus suggest that neurons within these frontal and parietal regions interact to drive the sustained neuronal firing associated with the maintenance of information. In a similar fashion, we found evidence for coupling between frontal and parietal BOLD activity when we examined performance-related increases in "functional connectivity" (Friston et al., 1997). Specifically, during the performance of correct compared to incorrect trials, increased functional connectivity was observed between the right IPS and a region extending forward from the right FEF to include both the superior frontal sulcus and the superior frontal gyrus/cingulate gyrus. Like the neurophysiological findings described above, these imaging results suggest that correct WM performance is not the result of activity in a single region but instead reflects the concerted activity of a network of regions, involving important parietofrontal interactions. Cornette et al. (2001) reached a similar conclusion when they examined the correlation between activity in the superior frontal sulcus and the SPL in a recent imaging study of WM for oriented gratings.

It is noteworthy that the network of regions exhibiting differential BOLD activity during the delay overlaps extensively with the spatial attention network (Kastner and Ungerleider, 2000; Mesulam, 1981). This finding is consistent with proposals that the two types of processes share many key neural substrates (Awh and Jonides, 2001; Desimone and Duncan, 1995; Mesulam, 1990).

#### Performance-Related BOLD Activity at Encoding

As shown in Figure 3A, two extrastriate visual areas exhibited stronger responses evoked by the sample stimulus on correct compared to incorrect trials: a dorsal occipital region on the middle occipital gyrus (BA 18/19) and an inferior temporal region (BA 37). The dorsal occipital region likely included the human homolog of area V3A (Tootell et al., 1997), which is highly selective for visual motion but also responds to texture (Kastner et al., 2000). Our activated region may also have included the human counterpart of monkey area V6, which is highly selective for oriented lines (Galletti et al., 1999). The inferior temporal region may be the same area activated in tasks involving successive orientation discrimination (Faillenot et al., 2001; Orban et al., 1997). In this connection, findings of related single-cell studies have suggested orientation-specific mechanisms in posterior parts of the inferior temporal cortex of monkeys (Vogels and Orban, 1994). Additionally, the fixed-effects analysis revealed that differential BOLD activity at encoding for correct compared to incorrect trials also occurred along the calcarine fissure, in early visual areas (V1/V2, BA 17/18) known to be highly responsive to oriented bars (e.g.,



Hubel and Wiesel, 1968). This differential activity suggests that very early processing stages also contribute to task performance.

The increased BOLD activity evoked by the sample stimulus at encoding observed in the regions of visual cortex described above is most likely due to attentional modulation in areas responsive to the visual stimuli we employed (Corbetta et al., 1991). Indeed, the difference in fMRI signal for correct compared to incorrect trials during encoding (Figure 3A) is highly reminiscent of the difference between attended and unattended conditions in both monkey single-cell as well as human ERP and imaging studies (for reviews, see Desimone and Duncan, 1995; Kastner and Ungerleider, 2000; Luck et al., 2000; Mangun et al., 2000). In those studies, however, subjects were explicitly instructed to attend to the stimulus on some trials and not to attend on others, whereas in our study, endogenous fluctuations in attention from trial to trial likely produced the response modulation.

It has previously been shown that increased attention leads not only to increased neuronal activity but also to improved performance. Spitzer et al. (1988) found that the responses of V4 cells increased to the same physical stimulus when the monkey performed a harder task, which required more attentional resources. Importantly, the increase in activity did not appear to correspond to a simple gain in signal but instead likely reflected an increase in response selectivity. A similar mechanism may underlie our results. For the dorsal occipital region, we observed that the boost in BOLD signal for correct relative to incorrect trials was greater during encoding than during retrieval (Figure 3A, left panel), suggesting increased selectivity at the time of encoding. Thus, we suggest that the increased stimulus evoked BOLD activity at encoding corresponds to increased neuronal processing associated with increased attention on correct trials; that is, increased neuronal processing leads to correct performance.

The differential BOLD signal observed during encoding in the present WM task is similar to the one reported by Brewer et al. (1998) and Wagner et al. (1998) for long-term memory. In those studies, it was shown that BOLD activity at the time of encoding predicted the subjects' ability to later remember the event.

#### Performance-Related Activity at Test

Several regions engaged by our WM task were more active for correct than incorrect trials at test, including very early areas in posterior cortex to anterior prefrontal regions. This is likely a reflection of the multiple computations taking place when the test stimulus is presented, such as visual processing of that stimulus, the matching operation involving the sample and test stimuli, as well as preparatory response processes. We found, in addition, that some of the regions with performance-related BOLD activity were selective for the test phase, including the anterior insula and the caudate and putamen (see Figure 3C). The latter two regions were likely involved in preparatory response processes. The anterior insula is a region of cortex activated in a host of paradigms, including attention (Gitelman et al., 1999; Hopfinger et al., 2000; LaBar et al., 1999) and WM (Courtney et al., 1997; LaBar et al., 1999) tasks. It is not clear, however, why it was only differentially involved at test in our task.

#### What Determines Successful WM Performance?

By definition, for a WM trial to be correct, the neural processes occurring during encoding, delay, and test must be executed successfully. To rule out the possibility that differential delay activity was a simple consequence of poor encoding, as might have been the case in some single-cell studies reporting weak or absent firing during incorrect trials, we performed additional analyses confined to only those trials with strong BOLD signals at encoding (Experimental Procedures). Both voxel-wise maps (fixed-effects analysis) and ROI-based comparisons (random-effects analysis) employing strong encoding trials revealed the same pattern of results obtained when we included all trials, irrespective of encoding strength. At the same time, the importance of strong encoding signals was demonstrated by our analysis of the distribution of delay signals for correct and incorrect trials. For the three ROIs we investigated (right IPS, right FEF, and left DLPFC), for strongly encoded trials, delay activity reliably predicted behavioral performance. For weakly encoded trials, by contrast, only the right IPS exhibited a predictive relationship between delay activity and performance. We suggest, therefore, that the significant difference we observed between correct and incorrect BOLD signals during the delay cannot be due to good versus poor encoding of the stimulus. Instead, we would argue that while strong delay signals in a WM task depend on the proper encoding of the stimulus, proper encoding per se does not lead to correct performance without sustained activity during the delay.

A related question is why it is the case that correct trials are associated with stronger BOLD activity during the delay when compared to incorrect trials. For example, it is conceivable that for incorrect trials the wrong kind of information (e.g., bar orientation) was "effectively" maintained. In this instance, both correct and incorrect trials would be associated with similar levels of BOLD activity during the delay. Although this may have happened in some trials of our WM task, the markedly different delay signals during correct and incorrect trials speak against the interpretation that incorrect information was held in mind. Instead, our results suggest that, consistent with results from single-cell studies, accurate performance was supported by strong sustained signals during the delay interval and that little information was held in mind during the delay on incorrect trials. The present discussion may help explain why Zarahn et al. (2000) did not find differential BOLD activity for correct and incorrect trials during the delay phase of a spatial WM task. It is possible that, in their task, subjects maintained information during the delay for both correct and incorrect trials; during incorrect trials, however, the wrong kind of information may have been maintained.

#### Concluding Remarks

Some recent studies have investigated the relationship between performance and fMRI signals. In one such study, Ress et al. (2000) attributed fluctuations in activity in V1, as inferred from the fMRI signal, to trial-to-trial fluctuations in attention, which they suggested accounted for the variability in behavioral performance on a target detection task. In a similar vein, we suggest

that increased BOLD activity corresponds to increased neuronal processing associated with increased attention on correct trials and that increased neuronal processing leads to correct performance. In other words, attention, neuronal activity, and behavioral performance are interrelated. Moreover, we attribute the coupling between brain activity and performance to trial-to-trial fluctuations in attention, such that variability in the subjects' attention leads to variability in neuronal responses, which, in turn, cause variability in performance. Fluctuations in attention may be apparent during all task phases, such that increased BOLD activity during encoding, delay, and test all predict correct performance.

## Experimental Procedures

### Subjects

Nine healthy subjects (five women, 22–36 years old) participated in the study, which was approved by the National Institute of Mental Health Institutional Review Board. All subjects were in good health with no past history of psychiatric or neurological disease and gave informed written consent. Subjects had normal or corrected-to-normal (with contact lenses) visual acuity.

### Visual Task

There were three experimental conditions: working memory (WM), fixation control (FC), and detection (DT; results related to this condition are not presented in this paper and will not be discussed further). Each run comprised 24 trials in random order (16 WM, 4 FC, and 4 DT), with each trial lasting 14 s. The stimuli employed in WM trials consisted of a fixation spot (0.2°) and eight bars (1°) positioned around fixation. The orientation of the bars was vertical, horizontal, and oblique (+45° or −45°), chosen randomly for each display. In each run, half of the WM trials (8/16) involved a single change in the visual display (i.e., on these nonmatch trials, one of the bars in the test display changed orientation compared to the sample display), and half did not involve a change (i.e., the sample and test displays were identical). Subjects participated in seven to ten runs, each lasting 5 min 36 s (with a 1–2 min rest period between runs). The temporal structure of the trials is indicated in Figure 1. In WM trials, after a 1 s fixation, a sample visual display was presented for 0.5 s, followed by a 6 s fixation, and a test display for 0.5 s. Subjects were then prompted by a display with the letter “m” (for memory) to indicate “same” or “different” by using two hand-held buttons (right and left hand, respectively). “Same” meant that the test matched the sample, and “different” meant that it did not match. Subjects also indicated the confidence level of their response by indicating “high” or “low” (right and left hand, respectively) when “c” appeared on the display. Each of the two response periods lasted 2 s. Finally, a blank screen terminated the trial, which lasted 2 s (intertrial interval). Subjects were instructed to maintain fixation for those displays with a fixation spot. FC trials did not have any maintenance demands. On these trials, subjects were instructed to maintain fixation and press both buttons in both response periods. Before the actual scan session, subjects underwent a practice session in which they performed five to six runs in order to become familiar with the task.

### MRI Data Acquisition

Images were acquired with a 3.0 Tesla GE Signa scanner (Milwaukee, WI) using a custom-made head coil (IGC-Medical Advances, Milwaukee, WI). Subjects were tested in a scanning session that lasted approximately 2 hr. Functional images were taken with a gradient echo echo-planar imaging sequence (TR = 2 s; TE = 30 ms; FOV = 24 cm; flip angle = 90°; 64 × 64 matrix). Whole-brain coverage was obtained with 32 sagittal slices (thickness, 5 mm; in-plane resolution, 3.75 × 3.75 mm). However, as in virtually all fMRI studies, susceptibility changes led to some signal attenuation in orbitofrontal and anterior medial temporal regions (i.e., at the level of the anterior amygdala), which are outside those that have been implicated in WM processes, as indicated by lesion, single-cell, or imaging studies; we

did not observe significant signal loss in the inferior frontal gyrus. Echo-planar images were coregistered to a high-resolution anatomical scan of the same subject's brain taken in the same session (3D SPRG, TR = 15 ms, TE = 5.4 ms, flip angle = 45°, 256 × 256 matrix, FOV = 24 cm, 124 sagittal slices, thickness, 1.2 mm).

Visual stimuli were generated on a PC and rear projected onto a translucent screen placed outside the bore of the magnet. Stimuli were viewed from inside the magnet via a mirror system attached to the head coil. The first scanner pulse of each functional run synchronized MR acquisition with visual presentation.

### Data Analysis

WM trials were sorted according to whether they were correct or incorrect and whether subjects reported high or low confidence. Trials in which the subjects did not respond at both response periods were discarded in subsequent analyses. All of the analyses reported here employed high-confidence trials only. In this fashion, the contribution from guessing was minimized.

Functional data were smoothed with an isotropic 8 mm Gaussian kernel (FWHM) and analyzed with multiple regression (Friston et al., 1995). An 8 mm kernel was employed to reduce the influence of anatomical variability among the individual maps (see below) in generating group maps. For the analyses, a set of box car regressors (mean corrected) were defined that were “on” (or positive) for the duration of the encoding and test task phases (i.e., the sample and test visual stimuli, respectively) and “off” (or zero) elsewhere. For the delay phase, the box car regressor was “on” for the last 2.5 s of the delay period (see below). The regressors were then convolved with a canonical hemodynamic impulse response function in order to account for response lag and dispersion (Cohen, 1997). The linear models also included a constant term and a linear term (for every run) that served as covariates of no interest (these terms controlled for drifts of MR signal across and within runs). Statistical hypotheses were tested via F tests of contrasts of interests. To delineate the network of brain regions involved in our WM task, WM and FC trials were contrasted (the respective regressors were “on” during the sample display, the delay interval, and the test display and were “off” elsewhere). For the performance analysis, correct and incorrect trials were compared at specific task phases.

We chose the delay regressor to consist of the last 2.5 s of the delay task period. This was because, as noted by D'Esposito and colleagues (Postle et al., 2000b; Zarahn et al., 1997), one concern in modeling BOLD activity during delay tasks is that neural activity associated with encoding might produce a hemodynamic response that extends into the subsequent delay period, leading to activity captured by the delay period covariate that is contaminated by encoding activity. Therefore, we have followed D'Esposito and colleagues's suggestion of separating the onset of the delay period covariate at least 4 s from the onset of encoding, which allows our analysis to statistically resolve temporally neighboring signals (see also Figure 2 of Zarahn et al., 1997, and associated discussion). It should be noted, however, that we also performed our analyses with a 6 s delay regressor, and the overall pattern of results did not change. The group maps looked virtually identical to those shown in Figure 3, and, as with the 2.5 s delay regressor, bilateral SPL, bilateral IPS, and right FEF were significant at the group level (random-effects analysis) for the delay component of the task.

We analyzed our results in two complementary ways: whole-brain voxel-wise (with AFNI; Cox, 1996) and ROI-based (with software developed by the authors in Matlab). Both voxel-wise and ROI-based analyses employed multiple regression. Statistical analyses of group results contrasting fMRI signals on correct and incorrect trials were performed on ROIs selected independently of task performance (random-effects analysis). These results were supplemented by a less exacting fixed-effects analysis performed on a voxel-wise manner that generated summary group Z maps. For the ROI analysis, a set of ROIs was defined on each individual's brain based on the network of regions involved in the WM task (the ROIs were drawn on original, i.e., not normalized, brains). These were regions activated in the WM versus FC contrast ( $p < 0.005$ , uncorrected). Two principles were employed to define the ROIs. First, we inspected individual maps (WM versus FC; Figure 2) for activation in regions demonstrated by other studies to be important for WM (e.g., Haxby et al.,

2000), including the DLPFC (anterior middle frontal gyrus), FEF, Pre-SMA, anterior cingulate, SPL, and IPS. Next, we inspected individual maps for other activations that were found consistently in at least four out of the nine subjects. These included the calcarine fissure, the dorsal occipital cortex, the inferior temporal gyrus, the anterior insula, and the posterior MFG. In all cases, we employed, as much as possible, anatomical landmarks to demarcate the ROIs (e.g., by drawing masks surrounding the posterior calcarine fissure).

For each ROI, representative time series were obtained by averaging the time series of the individual voxels within the ROI. Multiple regression was employed to estimate the contributions of BOLD signal during encoding, delay, and test for correct and incorrect trials. Random-effects group analyses were obtained by performing repeated measures ANOVAs or paired *t* tests where the dependent measures were individuals'  $\beta$  weights (i.e., least-squares parameter estimates ["weights"]) associated with the predictor variables [regressors] obtained by a multiple linear regression fit to the data) for the condition of interest (Table 1; for these group analyses, significance was set at  $p < 0.05$ ). For the fixed-effects analysis, statistical group maps were obtained by converting each individual's *F* map into a *Z* map and then combining these into a composite final *Z* map. For that purpose, each individual's brain was transformed with AFNI into the standard coordinate space of Talairach and Tournoux (1988). These transformed maps were then combined (averaged together and multiplied by the square root of the number of subjects). This type of analysis provides an assessment of the activations that are common to the group studied. In the figures, the results of this analysis are overlaid on high-resolution structural scans from a representative subject. Because the fixed-effect analysis is uncorrected for multiple comparisons, a more stringent *p* value of 0.0001 or less was chosen for significance.

To quantify the effect of task performance on signal strength, we developed a performance index for each task phase. We assessed the normalized difference between correct and incorrect trials for the encoding phase, for example, in the following manner:

$$I = [\beta(\text{correct}) - \beta(\text{incorrect})] / \max[\text{abs}(\beta(\text{correct})), \text{abs}(\beta(\text{incorrect}))]$$

where  $\beta(\text{correct})$  and  $\beta(\text{incorrect})$  refer to the estimated  $\beta$  weights (averaged across all subjects) for the encoding phase of the task. Corresponding indices were defined for the delay and matching phases of the task. We employed the above index, instead of the more standard " $(a - b)/(a + b)$ " index because a few average  $\beta$  weights for incorrect trials were negative. By using the max function in the denominator, the difference between correct and incorrect trials is normalized, as one would desire, by the size of the largest response (in absolute terms).

To quantify the contingency between fMRI amplitude and the subjects' performance, we employed a logistic regression. We fit a logistic function to the subjects' performance on each trial as a function of the fMRI signal amplitude on that trial. For each subject, the fMRI signal was defined as percent signal change of the raw BOLD signal (after correction for linear drift) relative to the mean of all scans for the ROI in question. The slope of the best-fitting logistic function measures the strength of the predictive effect. Data were combined across subjects, and the best-fit slope was determined (Figure 4) for each of the time points within a trial (i.e., 7 TRs) and tested for significance (whether reliably greater than zero). These signals were also used for the investigation of the distribution of delay activity (Figure 5), which was considered to be the signal at the 6th TR (10 s into the trial); encoding signals were considered to be the signal at the 4th TR (6 s into the trial); see Figure 4 for the timing of task phases.

We investigated how brain regions were coupled during correct and incorrect trials by testing for performance-dependent changes in "functional connectivity" (Friston et al., 1997). We tested for any such increase of functional connectivity with the right IPS by performing linear multiple regression. The key term of this analysis (also called "psychophysiological interaction" analysis) is an interaction term involving brain activity, *x*, and a psychological variable, *p*. For each subject, a time series associated with the IPS was used as a regressor associated with brain activity (*x*). This time series was

chosen from the peak voxel in the IPS for the contrast between correct and incorrect trials during the delay period. The psychological regressor *p* was defined by the difference of the regressors modeling the effect of correct and incorrect trials for the delay phase of the task. The regressor  $x \times p$  represents the effect of interest, namely, the interaction between activity in the right IPS and performance in the task. Significant fits for this regressor indicate a performance-specific change in the "connectivity" between IPS and the rest of the brain. This analysis was performed on all individuals and combined into a group map as specified above.

We also analyzed differential BOLD activity during the delay that was limited to only those trials in which robust or "effective" encoding occurred. To define effective encoding, we made the following assumptions. First, we considered signals from the dorsal occipital and inferior temporal ROIs, which were regions exhibiting robust differential activity at encoding (Figure 3A). Second, within these two regions, event activity was taken as the summed raw BOLD signal (once linear trends were removed) for the third, fourth, and fifth TRs of each trial. Note that according to the typical hemodynamic evolution (Bandettini, 1999; Cohen, 1997), the response to the sample stimulus should peak around the fourth TR (see Figure 3A). For each subject, of all the high-confidence WM trials, we selected roughly half of the trials with the highest BOLD signal as our criterion for effective encoding. In this manner, we guaranteed that, for every subject, only high-confidence WM trials in which BOLD activity during encoding was greater than the mean BOLD activity during encoding were employed.

#### Acknowledgments

We thank Jerzy Bodurka, Maura Furey, and Rene Hill for assistance with scanning; Jill Weisberg for assistance with scanning and AFNI; Djalma Pessoa for statistical advice; and Robert Desimone, Jim Haxby, Alex Martin, and Jill Weisberg for invaluable suggestions on an earlier version of the manuscript. This study was supported by the National Institute of Mental Health; Intramural Research Program.

Received: November 7, 2001

Revised: May 31, 2002

#### References

- Awh, E., and Jonides, J. (2001). Overlapping mechanisms of attention and spatial working memory. *Trends Cogn. Sci.* 5, 119–126.
- Bandettini, P.B. (1999). The temporal resolution of the functional MRI. In *Functional MRI*, C.T.W. Moonen and P.B. Bandettini, eds. (Berlin: Springer-Verlag), pp. 205–220.
- Bauer, R.H., and Fuster, J.M. (1976). Delayed-matching and delayed-response deficit from cooling dorsolateral prefrontal cortex in monkeys. *J. Comp. Physiol. Psychol.* 90, 293–302.
- Brewer, J.B., Zhao, Z., Desmond, J.E., Glover, G.H., and Gabrieli, J.D.E. (1998). Making memories: Brain activity that predicts how well visual experience will be remembered. *Science* 281, 1185–1187.
- Bruce, C.J., and Goldberg, M.E. (1985). Primate frontal eye fields. I. Single neurons discharging before saccades. *J. Neurophysiol.* 53, 603–635.
- Cabeza, R., and Nyberg, L. (2000). Imaging cognition II: An empirical review of 275 PET and fMRI studies. *J. Cogn. Neurosci.* 12, 1–47.
- Chafee, M.V., and Goldman-Rakic, P.S. (1998). Matching patterns of activity in primate prefrontal area 8a and parietal area 7ip neurons during a spatial working memory task. *J. Neurophysiol.* 79, 2919–2940.
- Chafee, M.V., and Goldman-Rakic, P.S. (2000). Inactivation of parietal and prefrontal cortex reveals interdependence of neural activity during memory-guided saccades. *J. Neurophysiol.* 83, 1550–1566.
- Chelazzi, L., Duncan, J., Miller, E.K., and Desimone, R. (1998). Responses of neurons in inferior temporal cortex during memory-guided visual search. *J. Neurophysiol.* 80, 2918–2940.
- Cohen, M.S. (1997). Parametric analysis of fMRI data using linear systems methods. *Neuroimage* 6, 93–103.
- Cohen, J.D., Perlstein, W.M., Braver, T.S., Nystrom, L.E., Noll, D.C.,

- Jonides, J., and Smith, E.E. (1997). Temporal dynamics of brain activation during a working memory task. *Nature* 386, 604–608.
- Corbetta, M., Miezin, F.M., Dobmeyer, S., Shulman, G.L., and Petersen, S.E. (1991). Selective and divided attention during visual discriminations of shape, color, and speed: functional anatomy by positron emission tomography. *J. Neurosci.* 11, 2383–2402.
- Cornette, L., Dupont, P., Salmon, E., and Orban, G.A. (2001). The neural substrate of orientation working memory. *J. Cogn. Neurosci.* 13, 813–828.
- Courtney, S.M., Ungerleider, L.G., Keil, K., and Haxby, J.V. (1996). Object and spatial visual working memory activate separate neural systems in human cortex. *Cereb. Cortex* 6, 39–49.
- Courtney, S.M., Ungerleider, L.G., Keil, K., and Haxby, J.V. (1997). Transient and sustained activity in a distributed neural system for human working memory. *Nature* 386, 608–611.
- Courtney, S.M., Petit, L., Maisog, J.M., Ungerleider, L.G., and Haxby, J.V. (1998). An area specialized for spatial working memory in human frontal cortex. *Science* 279, 1347–1351.
- Cox, R.W. (1996). AFNI: Software for analysis and visualization of functional magnetic resonance neuroimages. *Comput. Biomed. Res.* 29, 162–173.
- Desimone, R., and Duncan, J. (1995). Neural mechanisms of selective visual attention. *Annu. Rev. Neurosci.* 18, 193–222.
- D'Esposito, M. (2001). Functional neuroimaging of working memory. In *Handbook of Functional Neuroimaging of Cognition*, R. Cabeza, and A. Kingstone, eds. (Cambridge, MA: The MIT Press), pp. 293–327.
- D'Esposito, M., Aguirre, G.K., Zarahn, E., Ballard, D., Shin, R.K., and Lease, J. (1998). Functional MRI studies of spatial and nonspatial working memory. *Cogn. Brain Res.* 7, 1–13.
- Faillenot, I., Sunaert, S., Van Hecke, P., and Orban, G.A. (2001). Orientation discrimination of objects and gratings compared: an fMRI study. *Eur. J. Neurosci.* 13, 585–596.
- Friston, K.J., Holmes, A.P., Worsley, K.J., Poline, J.P., Heather, J.D., and Frackowiak, R.S. (1995). Statistical parametric maps in functional imaging: a general linear approach. *Hum. Brain Mapp.* 3, 165–189.
- Friston, K.J., Buechel, C., Fink, G., Morris, J.S., Rolls, E.T., and Dolan, R.J. (1997). Psychophysiological and modulatory interactions in neuroimaging. *Neuroimage* 6, 218–229.
- Funahashi, S., Bruce, S.J., and Goldman-Rakic, P.S. (1989). Mnemonic coding of visual space in the monkey's dorsolateral prefrontal cortex. *J. Neurophysiol.* 61, 1–19.
- Funahashi, S., Bruce, C.J., and Goldman-Rakic, P.S. (1993). Dorsolateral prefrontal lesions and oculomotor delayed-response performance: evidence for mnemonic "scotomas." *J. Neurosci.* 13, 1479–1497.
- Fuster, J.M. (1973). Unit activity in prefrontal cortex during delayed-response performance: neuronal correlates of transient memory. *J. Neurophysiol.* 36, 61–78.
- Fuster, J.M. (1997). *The Prefrontal Cortex*, Third edition (Philadelphia, PA: Lippincott-Raven).
- Fuster, J.M. (2001). The prefrontal cortex—an update: time is of the essence. *Neuron* 30, 319–333.
- Fuster, J.M., and Alexander, G.E. (1971). Neuron activity related to short-term memory. *Science* 173, 652–654.
- Fuster, J.M., and Jervey, J.P. (1982). Neuronal firing in the infero-temporal cortex of the monkey in a visual memory task. *J. Neurosci.* 2, 361–375.
- Fuster, J.M., Bodner, M., and Kroger, J.K. (2000). Cross-modal and cross-temporal association in neurons of frontal cortex. *Nature* 405, 347–351.
- Galletti, C., Fattori, P., Gamberini, M., and Kutz, D.F. (1999). The cortical visual area V6: brain location and visual topography. *Eur. J. Neurosci.* 11, 3922–3936.
- Gitelman, D.R., Nobre, A.C., Parrish, T.B., LaBar, K.S., Kim, Y.H., Meyer, J.R., and Mesulam, M. (1999). A large-scale distributed network for covert spatial attention: further anatomical delineation based on stringent behavioural and cognitive controls. *Brain* 122, 1093–1106.
- Goldman, P.S., and Rosvold, H.E. (1970). Localization of function within the dorsolateral prefrontal cortex of the rhesus monkey. *Exp. Neurol.* 27, 291–304.
- Goldman-Rakic, P.S. (1995). Cellular basis of working memory. *Neuron* 14, 477–485.
- Haxby, J.V., Petit, L., Ungerleider, L.G., and Courtney, S.M. (2000). Distinguishing the functional roles of multiple regions in distributed neural systems for visual working memory. *Neuroimage* 11, 380–391.
- Hopfinger, J.B., Buonocore, M.H., and Mangun, G.R. (2000). The neural mechanisms of top-down attentional control. *Nat. Neurosci.* 3, 284–291.
- Hubel, D.H., and Wiesel, T.N. (1968). Receptive fields and functional architecture of monkey striate cortex. *J. Physiol.* 195, 215–243.
- Jonides, J., Smith, E.E., Koeppe, R.A., Awh, E., Minoshima, S., and Mintun, M.A. (1993). Spatial working memory in humans as revealed by PET. *Nature* 363, 623–625.
- Jonides, J., Schumacher, E.H., Smith, E.E., Koeppe, R.A., Awh, E., Reuter-Lorenz, P.A., Marshuetz, C., and Willis, C.R. (1998). The role of parietal cortex in verbal working memory. *J. Neurosci.* 18, 5026–5034.
- Kastner, S., and Ungerleider, L.G. (2000). Mechanisms of visual attention in the human cortex. *Annu. Rev. Neurosci.* 23, 315–341.
- Kastner, S., De Weerd, P., and Ungerleider, L.G. (2000). Texture segregation in the human visual cortex: A functional MRI study. *J. Neurophysiol.* 83, 2453–2457.
- Kubota, K., and Niki, H. (1971). Prefrontal cortical unit activity and delayed alternation performance in monkeys. *J. Neurophysiol.* 34, 337–347.
- LaBar, K.S., Gitelman, D.R., Parrish, T.B., and Mesulam, M. (1999). Neuroanatomic overlap of working memory and spatial attention networks: a functional MRI comparison within subjects. *Neuroimage* 10, 695–704.
- Luck, S.J., Woodman, G.F., and Vogel, E.K. (2000). Event-related potential studies of attention. *Trends Cogn. Sci.* 4, 432–440.
- Mangun, G.R., Hopfinger, J.B., and Jha, A.P. (2000). Integrating electrophysiology and neuroimaging in the study of brain function. *Adv. Neurol.* 84, 35–49.
- Mesulam, M.M. (1981). A cortical network for directed attention and unilateral neglect. *Ann. Neurol.* 10, 309–325.
- Mesulam, M.M. (1990). Large-scale neurocognitive networks and distributed processing for attention, language, and memory. *Ann. Neurol.* 28, 597–613.
- Miller, E.K., Erikson, C.A., and Desimone, R. (1996). Neural mechanisms of visual working memory in prefrontal cortex of the macaque. *J. Neurosci.* 16, 5154–5167.
- Orban, G.A., Dupont, P., Vogels, R., Bormans, G., and Mortelmans, L. (1997). Human brain activity related to orientation discrimination tasks. *Eur. J. Neurosci.* 9, 246–259.
- Petit, L., Courtney, S.M., Ungerleider, L.G., and Haxby, J.V. (1998). Sustained activity in the medial wall during working memory delays. *J. Neurosci.* 18, 9429–9437.
- Picard, N., and Strick, P.L. (1996). Motor areas of the medial wall: a review of their location and functional activation. *Cereb. Cortex* 6, 342–353.
- Postle, B.R., Berger, J.S., Taich, A.M., and D'Esposito, M. (2000a). Activity in human frontal cortex associated with spatial working memory and saccadic behavior. *J. Cogn. Neurosci.* 12, 2–14.
- Postle, B.R., Zarahn, E., and D'Esposito, M. (2000b). Using event-related fMRI to assess delay-period activity during performance of spatial and nonspatial working memory tasks. *Brain Res. Brain Res. Protoc.* 5, 57–66.
- Ress, D., Backus, B.T., and Heeger, D.J. (2000). Activity in primary visual cortex predicts performance in a visual detection task. *Nat. Neurosci.* 3, 940–945.
- Rosenkilde, C.E., Bauer, R.H., and Fuster, J.M. (1981). Single cell

activity in ventral prefrontal cortex of behaving monkeys. *Brain Res.* 209, 375–394.

Rowe, B.R., Toni, I., Josephs, O., Frackowiak, R.S., and Passingham, R.E. (2000). The prefrontal cortex: response selection or maintenance within working memory? *Science* 288, 1656–1660.

Sakai, K., Rowe, J.B., and Passingham, R.E. (2002). Active maintenance in prefrontal area 46 creates distractor-resistant memory. *Nat. Neurosci.* 5, 479–484.

Smith, E.E., Jonides, J.J., Koeppe, R.A., Awh, E., Schumacher, E.H., and Minoshima, S. (1995). Spatial versus object working memory: PET investigations. *J. Cogn. Neurosci.* 7, 337–356.

Spitzer, H., Desimone, R., and Moran, J. (1988). Increased attention enhances both behavioral and neuronal performance. *Science* 240, 338–340.

Talairach, J., and Tournoux, P. (1988). *Co-planar Stereotaxis Atlas of the Human Brain*, M. Rayport, transl. (New York: Thieme Medical).

Tootell, R.B., Mendola, J.D., Hadjikhani, N.K., Ledden, P.J., Liu, A.K., Reppas, J.B., Sereno, M.I., and Dale, A.M. (1997). Functional analysis of V3A and related areas in human visual cortex. *J. Neurosci.* 17, 7060–7078.

Vogels, R., and Orban, G.A. (1994). Activity of inferior temporal neurons during orientation discrimination with successively presented gratings. *J. Neurophysiol.* 71, 1428–1451.

Wagner, A.D., Schacter, D.L., Rotte, M., Koustaal, W., Maril, A., Dale, A.M., and Rosen, B.R. (1998). Building memories: Remembering and forgetting of verbal experiences as predicted by brain activity. *Science* 281, 1188–1191.

Watanabe, M. (1986a). Prefrontal unit activity during delayed conditional go/no-go discrimination in the monkey I. Relation to the stimulus. *Brain Res.* 382, 1–14.

Watanabe, M. (1986b). Prefrontal unit activity during delayed conditional go/no-go discrimination in the monkey I. Relation to go and no-go responses. *Brain Res.* 382, 15–27.

Zarahn, E., Aguirre, G., and D'Esposito, M. (1997). A trial-based experimental design for fMRI. *Neuroimage* 6, 122–138.

Zarahn, E., Aguirre, G., and D'Esposito, M. (2000). Replication and further studies of neural mechanisms of spatial mnemonic processing in humans. *Brain Res. Cogn. Brain Res.* 9, 1–17.